Identification of the vinculin-binding site in the cytoskeletal protein α-actinin

Alistair McGREGOR, Andrew D. BLANCHARD,* Arthur J. ROWE and David R. CRITCHLEY
Department of Biochemistry, University of Leicester, Leicester LE1 7RH, U.K.

Using low-speed sedimentation equilibrium we have established that vinculin binds to α-actinin with a K_d of 1.3×10^{-5} M. Electron microscopy of negatively stained preparations of vinculin revealed spherical particles (diameter 11.2 nm; S.D. 1.7 nm, $n = 21$), whereas α-actinin appeared as a rod-shaped particle (length 33 nm; S.D. 3.3 nm, $n = 23$). Mixtures of the two proteins contained both 'lollipop'- and 'dumbell'-shaped particles which we interpret as either one or two spherical vinculin molecules associated with the ends of the α-actinin rod. We have further defined the vinculin-binding site in α-actinin using ^{125}I-vinculin and a gel-blot assay in which proteolytic fragments of α-actinin and fragments of α-actinin expressed in *Escherichia coli* were resolved by SDS/PAGE and blotted to nitrocellulose. ^{125}I-vinculin bound to polypeptides derived from the spectrin-like repeat region of α-actinin, but did not bind to the actin-binding domain. Binding was inhibited by a 100-fold molar excess of unlabelled vinculin. Using a series of glutathione S-transferase fusion proteins we have mapped the vinculin-binding site to a region toward the C-terminal end of the molecule (α-actinin residues 713–749). ^{125}I-vinculin also bound to fusion proteins containing this sequence which had been immobilized on glutathione–agarose beads. The vinculin-binding site is localized in a highly conserved region of the molecule close to the first of two EF-hand calcium-binding motifs.

INTRODUCTION

α-Actinin is a rod-shaped dimeric F-actin bundling protein found in muscle and non-muscle cells at sites where actin is attached to cytoplasmic and membrane-associated structures (reviewed by Blanchard et al., 1989). Thus α-actinin is one of a number of cytoskeletal proteins found in cell–cell and cell–extracellular-matrix adherens-type junctions, where it is thought to link the cytoplasmic domain of adhesion receptors of the cadherin and integrin families to the actin cytoskeleton (Burridge et al., 1988; Luna and Hitt, 1992). In both cell–cell and cell–matrix junctions, α-actinin co-localizes with the cytoskeletal protein vinculin, and an interaction between these two proteins is envisaged to be central to the pathway linking adhesion receptors to filamentous actin.

Evidence that α-actinin binds to vinculin has stemmed largely from experiments in which α-actinin resolved by SDS/PAGE and transferred to nitrocellulose has been shown to bind ^{125}I-labelled vinculin (Otto, 1983; Wilkins et al., 1983). Similarly, ^{125}I-labelled α-actinin has been shown to bind to vinculin using the same gel-blot assay (Belkin and Koteliansky, 1987), although in neither case was it shown that the unlabelled ligand could inhibit binding. Further biochemical evidence in support of an interaction between α-actinin and vinculin has come from studies using fluorescence energy transfer, from which a K_d of 2.2×10^{-6} M was derived (Wacchstock et al., 1987). The same authors also showed that vinculin was eluted slightly earlier from a gel-filtration column when the column was pre-equilibrated with α-actinin, a result consistent with an interaction between these two proteins.

The primary sequence of a number of α-actinin isoforms has now been determined (Baron et al., 1987a; Noegel et al., 1987; Arimura et al., 1988; Fyrberg et al., 1990; Beggs et al., 1992; Parr et al., 1992; Waites et al., 1992), and considerable progress has been made in defining the domain structure of the protein (Blanchard et al., 1989). The actin-binding domain in α-actinin has been localized to the N-terminal region of the protein (Mimura and Asano, 1986; Baron et al., 1987a), and we have recently provided evidence that residues 120–134 contain an actin-binding site (Hemmings et al., 1992; Kuhlman et al., 1992). The N-terminal domain also appears to contain a binding site for the 82 kDa cytoskeletal protein zyxin, which co-localizes with α-actinin and vinculin in adherens junctions (Crawford et al., 1992). The central region of α-actinin is composed of four spectrin-like repeats (Baron et al., 1987a; Davison et al., 1989) responsible for the rod-shape of the molecule (3–4 nm × 30–40 nm) and the formation of the α-actinin anti-parallel dimer (Imamura et al., 1988). This region of the molecule is thought to contain binding sites for the cytoplasmic domains of the β1 and β3 subunits of integrins (Otey et al., 1990), providing a possible route linking integrins to F-actin. Finally, the C-terminal domain of α-actinin contains two EF-hand calcium-binding motifs which accounts for the ability of calcium to inhibit binding of the non-muscle α-actinin isoforms to F-actin (Burridge and Feramisco 1981; Bennett et al., 1984; Duhaiman and Bamburg, 1984; Landon et al., 1985; Witke et al., 1993).

In the present study we have characterized the interaction between vinculin and α-actinin using low-speed equilibrium sedimentation and electron microscopy, and have identified a vinculin-binding site in α-actinin using recombinant α-actinin polypeptides expressed in *Escherichia coli.*

MATERIALS AND METHODS

Purification of vinculin and α-actinin

Vinculin was purified from chicken gizzard according to the method of O'Halloran et al. (1986). α-Actinin was purified from the same source, essentially as described by Feramisco and Burridge (1980), but using DEAE-Sepharose Fast Flow and Superdex 200 Prep Grade columns (Pharmacia) instead of DE-52 and Sepharose 6B-Cl. Final purification was achieved using a Q-Sepharose column (2.6 cm × 10 cm) packed and loaded in 20 mM Tris/acetate buffer (pH 7.6)/20 mM NaCl/0.1 mM

Abbreviations used: GST, glutathione S-transferase; $\overline{M}_w$, weight-averaged molecular mass.
* Present address: Department of Biochemistry, University of Oxford, Oxford OX1 3QU, U.K.

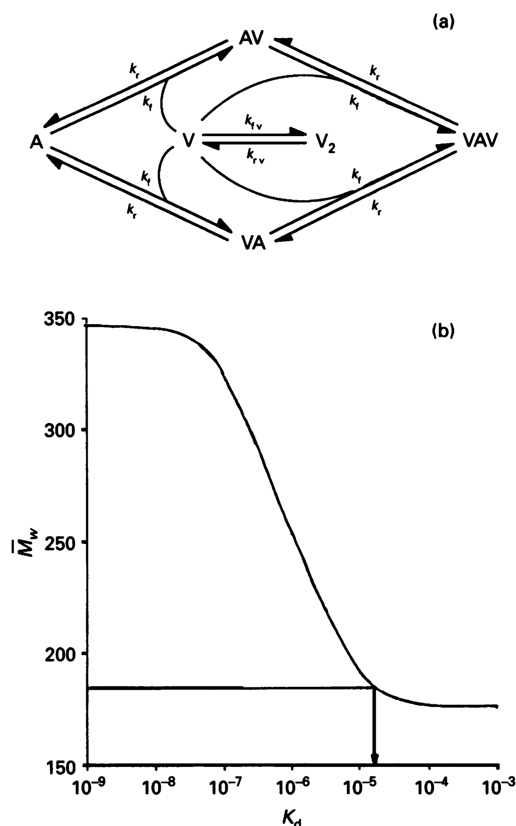

Figure 1 (a) Model of the actinin–vinculin interaction and (b) $\bar{M}_w$–K_d plot

(**a**) Model of the interaction between α-actinin and vinculin analysed using the STELLA modelling package. The components denoted are: A, α-actinin dimer; V, vinculin monomer; AV and VA, α-actinin dimer with one molecule of vinculin bound; VAV, α-actinin dimer complexed with two vinculin molecules; V_2, vinculin dimers. The equilibrium constants for the various steps in the interaction between the two proteins are defined by k_f and k_r, the forward and reverse rate constants. k_{fv} and k_{rv} are the forward and reverse rate constants of vinculin dimerization. (**b**) A graph showing the expected $\bar{M}_w$ of an α-actinin/vinculin mixture as a function of K_d generated using the STELLA modelling package. In the example shown, the concentrations of α-actinin and vinculin were 0.715 μM and 0.767 μM respectively. The experimentally determined value for $\bar{M}_w$ was 187 kDa, and the K_d value for the interaction between α-actinin and vinculin estimated from the graph is 1.3×10^{-5} M.

EDTA/0.1 % β-mercaptoethanol and eluted with a 200–350 mM NaCl gradient (250 ml).

Determination of a binding constant for the interaction between α-actinin and vinculin by low-speed sedimentation equilibrium

The weight-averaged molecular mass ($\bar{M}_w$) of an associating system characterized by a single interaction constant is determined solely by the molecular masses of the individual components and by the interaction constant (K_d). If the former values are known, then the latter can be determined. On this basis, we have developed a method for estimating the K_d of the interaction between α-actinin and vinculin using values for $\bar{M}_w$ determined by low-speed sedimentation equilibrium and the STELLA (High Performance Systems, Lyme, NH, U.S.A.) modelling package (Rowe, 1988). However, modelling of the α-actinin–vinculin interaction is not straightforward. Five macromolecular species will be present in solution: vinculin monomers, vinculin dimers, α-actinin dimers and α-actinin dimers, with either one or two molecules of vinculin bound. Three equilibrium constants will affect the final value for $\bar{M}_w$: that for vinculin self-association, that for formation of the α-actinin dimer with one molecule of vinculin bound, and that for formation of the α-actinin dimer with two molecules of vinculin bound (Figure 1a). Since only one variable parameter can be determined, we have calculated the self-association constant of vinculin from the $\bar{M}_w$ of vinculin determined under conditions identical with those used to study the formation of the α-actinin–vinculin complex. In the absence of information to suggest otherwise, it was assumed that the other two binding constants were equal and independent. Initially the concentrations of the five macromolecular species were estimated using the STELLA modelling package with a range of assumed K_d values and a knowledge of the total concentration of vinculin and α-actinin. A theoretical curve of $\bar{M}_w$ for an α-actinin/vinculin mixture as a function of K_d was then constructed (Figure 1b). Copies of the STELLA written worksheet are available from D.R.C. on request.

The $\bar{M}_w$ was determined for purified α-actinin and vinculin alone and for α-actinin/vinculin mixtures using standard techniques (Rowe, 1984). After sedimentation to low-speed equilibrium at 4 °C in a MSE Centriscan-75 analytical ultracentrifuge at 10600 rev./min, radial density scans were recorded at 280 nm. After acceleration to 50000 rev./min a further scan was taken 1 h later to provide an accurate baseline. The data were digitized using a graphics tablet linked to a microcomputer. The $\bar{M}_w$ across the geometrical midpoint of the cell, where all components are conserved at their cell-loading concentrations (Van Holde and Baldwin, 1958), was evaluated using values for the partial specific volume computed from the amino acid composition of the two proteins (Rowe, 1984). The K_d of the interaction was deduced by extrapolation on the theoretical curve (Figure 1b) using the $\bar{M}_w$ for the α-actinin/vinculin mixture determined by centrifugation.

Electron microscopy of α-actinin and vinculin

Samples of the proteins in 20 mM Tris/acetate (pH 7.6)/150 mM KCl/0.1 mM EDTA/0.1 % β-mercaptoethanol were negatively stained on glow-discharged celloidin–carbon support films, with saturated uranyl acetate applied after vapour fixation for 2 min above a 30 % glutaraldehyde solution. Protein concentrations of 0.2–0.5 μM were employed. The specimens were then examined in a JEOL 100CX transmission electron microscope. The instrumental magnification was calibrated using a diffraction grating replica.

Protein iodination

Vinculin (1 mg/ml) was dialysed into 50 mM sodium phosphate buffer, pH 8.0, containing 1 mM EDTA and 0.5 mM dithiothreitol. A 1 mg portion of vinculin was incubated with 500 μCi of Bolton and Hunter reagent (*N*-succinimidyl 3-(4-hydroxy-5-[^{125}I]iodophenyl) proprionate (Amersham) on ice for 30 min, and unincorporated label was removed either by extensive dialysis or gel filtration. The specific activity of the ^{125}I-labelled vinculin was between 20000 and 130000 c.p.m./μg, and analysis of the labelled protein by SDS/PAGE and autoadiography showed a single band coincident with vinculin detected by Coomassie Blue staining (results not shown).

Expression of α-actinin polypeptides in *E. coli*

Residues 1–269 of α-actinin, a region which contains the actin-binding domain, was expressed from an *Nco*I–*Hinc*II DNA

restriction endonuclease fragment derived from the chick smooth-muscle α-actinin cDNA C17 (Baron et al., 1987a). The fragment was subcloned into the *Nco*I–*Stu*I sites of the pMW172 expression vector (Way et al., 1990) and the construct transformed into *E. coli* strain BL21 (DE3). Cultures (1 litre) were grown at 37 °C to an attenuance at 600 nm of 0.5, expression of the protein was induced by addition of 0.01 mM isopropyl thiogalactoside, and cells were grown for a further 3–5 h at 30 °C. Cell pellets were resuspended in 12 mM sodium phosphate buffer, pH 7.3, containing 0.15 M NaCl and 5 mM EDTA and the proteinase inhibitors E64 (5 μM), leupeptin (10 μM) and phenylmethanesulphonyl fluoride (1 mM) (all from Sigma) prior to addition of Triton X-100 [1% (v/v) final concn.]. Cells were sonicated on ice (2 × 45 s), cell debris was pelleted at 8000 *g* × 15 min and the supernatant dialysed against 10 mM Tris/acetate (pH 7.6)/10 mM NaCl/2 mM EDTA/0.5% β-mercaptoethanol. The dialysed sample was applied to a DEAE-Sepharose Fast-Flow column (1 cm × 20 cm) in the same buffer, and proteins were eluted (30 ml/h) with a 150 ml linear salt gradient (10–15 mM). The expressed actin-binding domain was further purified using a Sephadex G-75 column (1 cm × 70 cm) eluted with the Tris/acetate buffer pH 7.6, and a hydroxyapatite column (0.5 cm × 3 cm) eluted with a gradient (50 ml) of 10–150 mM potassium phosphate buffer, pH 7.0.

An α-actinin polypeptide spanning residues 218–749 and containing all four spectrin-like repeats was expressed as a fusion protein with glutathione *S*-transferase (GST) using the pGEX vector (Pharmacia). Initially, an *Eco*RV–*Xmn*I restriction-enzyme fragment of the partial chick α-actinin cDNA clone C18 (Baron et al., 1987b) was subloned into the *Sma*I site of pGEX3, but the fusion protein was unstable, owing to cleavage between α-actinin residues Met-239 and Thr-240. This problem was overcome by deleting the nucleotides encoding residues 238–241 (Ile-Met-Thr-Tyr) by mutagenesis following standard procedures (Sambrook et al., 1989). This modified cDNA (GST/218–749*) was also used as a template to generate constructs in which nucleotides encoding each of the four repeats had been deleted (ΔR1–ΔR4) by mutagenesis. All mutants were authenticated by dideoxy sequencing prior to subcloning the *Eco*RV–*Xmn*I fragment into pGEX3. All additional α-actinin cDNAs were generated by PCR using 5′ primers containing a *Bam*HI site and 3′ primers containing an *Eco*RI site following standard procedures (Sambrook et al., 1989). PCR products were ethanol-precipitated, cut with *Bam*HI and *Eco*RI, gel-purified, and subcloned into the appropriate pGEX vector. The 5′ and 3′ ends of all pGEX constructs were sequenced using pGEX oligonucleotide primers. pGEX constructs were transformed into *E. coli* strain JM101, and cultures were grown to an attenuance at 600 nm of 0.5. Expression of fusion proteins was induced by the addition of 0.5 mM isopropyl thiogalactoside, and the cells were harvested after a further 3 h growth at 37 °C.

^{125}I-vinculin binding to α-actinin and α-actinin fusion proteins using a gel-blot assay

α-Actinin, α-actinin polypeptides liberated by thermolysin cleavage and *E. coli* cell lysates containing expressed α-actinin fusion proteins were resolved by SDS/PAGE and electroblotted on to nitrocellulose. Filters were incubated for 1 h in 25 mM Tris (pH 7.5)./0.15 M NaCl/0.2% Tween 20/1 mM EDTA/4% dried milk, and then for a further 12 h at room temperature in the same buffer (5 ml), either containing ^{125}I-vinculin or ^{125}I-vinculin plus unlabelled vinculin. Filters were then washed with 25 mM Tris (pH 7.5)/0.15 M NaCl (2 × 10 ml) for a total of 10 min, air-dried and bound ^{125}I-vinculin was detected by autoradiography.

Thermolysin cleavage of α-actinin

α-Actinin was dialysed into 0.1 M ammonium bicarbonate/5 mM $CaCl_2$, pH 7.6. The thermolysin (type X proteinase from *Bacillus thermoproteolyticus rokko*) (Sigma) was pre-activated 30 min before use by diluting a 20 mg/ml stock solution 1:20 with 1 mM $CaCl_2$. Incubations were carried out at 37 °C, and the reaction was stopped by the addition of 10 mM EDTA.

Binding of ^{125}I-vinculin to α-actinin GST fusion proteins adsorbed to glutathione–agarose beads

α-Actinin–GST fusion proteins were expressed in *E. coli* (50–100 ml cultures) and purified exactly as described by Smith and Johnson (1988), using 350 μl of glutathione–agarose beads (50% v/v) suspended in 12 mM phosphate buffer (pH 7.3)/0.15 M NaCl. The following proteinase inhibitors were added to buffers during purification of the fusion proteins; 5 mM EDTA, 5 μM E64 and 10 μM leupeptin and 1 mM phenylmethanesulphonyl fluoride. Beads with bound fusion proteins were incubated (3 h) in phosphate buffer containing 0.1% Triton X-100 and 3% BSA to block protein-binding sites. Aliquots of the beads containing approx. 50 μg of bound fusion protein were then incubated overnight in the same buffer (300 μl) containing ^{125}I-vinculin. Beads were collected by centrifugation, washed five times with buffer alone, and the amount of labelled vinculin bound determined using a Beckmann Gamma 5500 counter.

RESULTS

Determination of the K_d for the vinculin–α-actinin interaction by sedimentation equilibrium

Although the weight-averaged molecular mass ($\bar{M}_w$) for α-actinin (206 kDa) determined by sedimentation equilibrium was close to that expected for the dimer (Baron et al., 1987a), the experimental value for vinculin (131–136 kDa) was found to be appreciably and consistently higher than the formula mass (117 kDa; Price et al., 1989). It has been suggested (Milam, 1985) that vinculin may undergo a degree of reversible self-association in solution. From the $\bar{M}_w$ value obtained here, a K_d of 10^{-5} M was calculated for vinculin dimer formation as described in the Materials and methods section. The value of $\bar{M}_w$ for a solution containing near equimolar amounts of vinculin and α-actinin was 187 kDa. The K_d for the α-actinin–vinculin interaction calculated using this value was 1.3×10^{-5} M. From a consideration of the relationship between $\bar{M}_w$ and K_d (Figure 1b), a K_d value $\geqslant 4 \times 10^{-4}$ M would be indicative of negligible association, and hence our estimate shows evidence of a weak, but clearly measurable, interaction between the two proteins. This value for K_d is some six-fold higher than that reported previously (2.2×10^{-6} M; Wacchstock et al., 1987). However, the salt conditions employed were not identical, and this may have some effect on the binding interaction (Wacchstock et al., 1987).

Electron microscopy of α-actinin, vinculin and the α-actinin–vinculin complex

α-Actinin (0.25 μM) showed (Figure 2, panel A) rods of length 33 nm (S.D. = 3.3 nm, $n = 23$). Occasionally, bulbous ends (arrowed) could be discerned. These dimensions are within the range previously reported (30–40 nm) (Podlubnaya et al., 1985; Suzuki et al., 1976; Bretscher et al., 1979; Bennett et al., 1984;

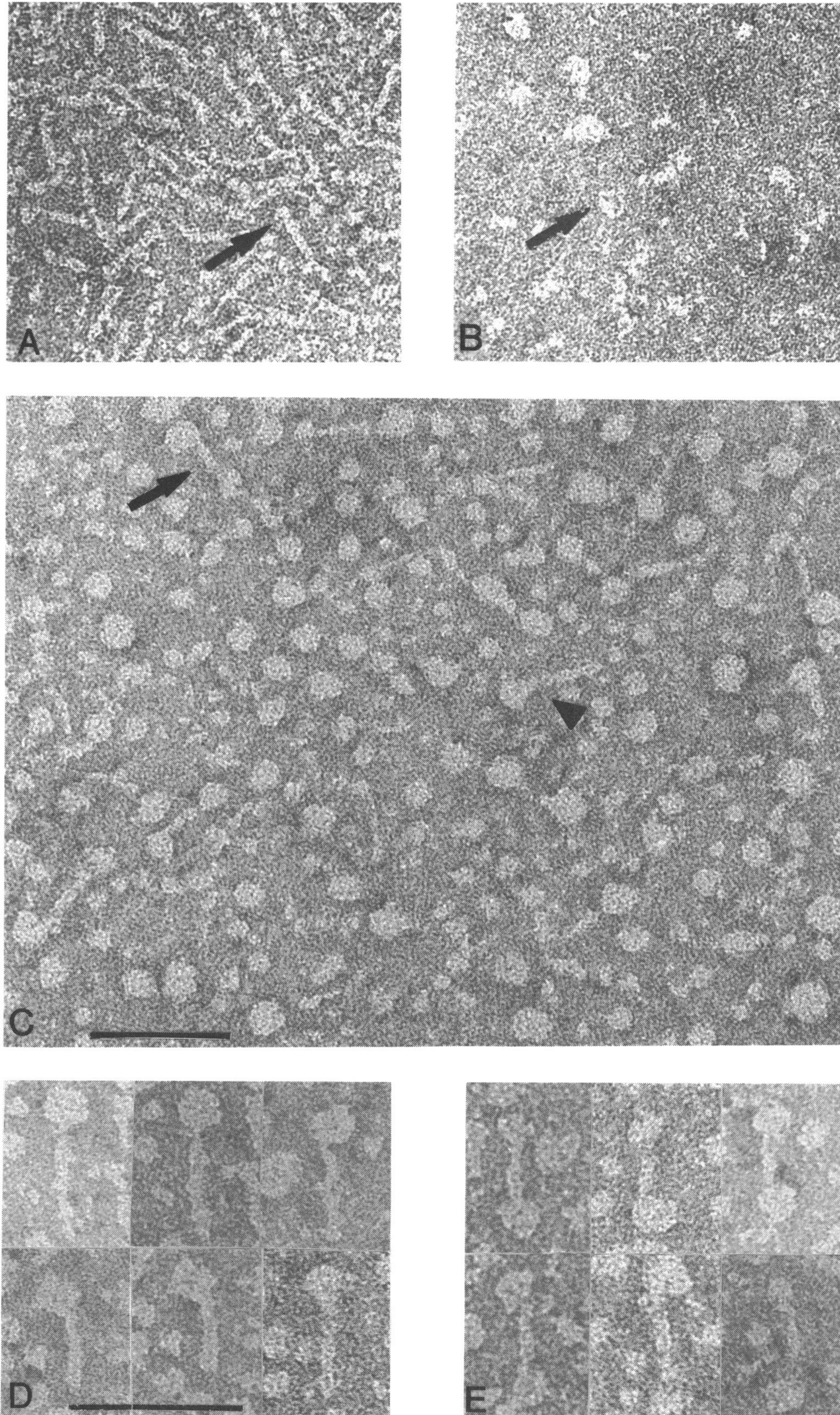

Figure 2 Electron microscopy of α-actinin, vinculin and of mixtures of the two proteins

Electron micrographs of negatively stained preparations of (panel A) α-actinin, (panel B) vinculin, and (panel C) a mixture of α-actinin and vinculin in a molar ratio of 1:2. (Panel A) the field shows a large number of linear α-actinin molecules, with a slight indication of bulbous ends (arrowed). (Panel B) the majority of the vinculin molecules seen are roughly spherical, with a small number showing a tail structure. Penetration of stain into the centre of the particles is seen in some cases (arrowed). (Panel C) The linear structures which are presumed to be α-actinin can often be observed to have either one (arrowhead) or two (arrow) spherical vinculin molecules attached to their extremities. (Panels D and E) montages of the structures designated as 'lollipops' (panel D) or 'dumbells' (panel E); see the text. The bar is 50 nm. The magnifications in panels A–C are identical. Similarly the magnifications in panels D and E are the same.

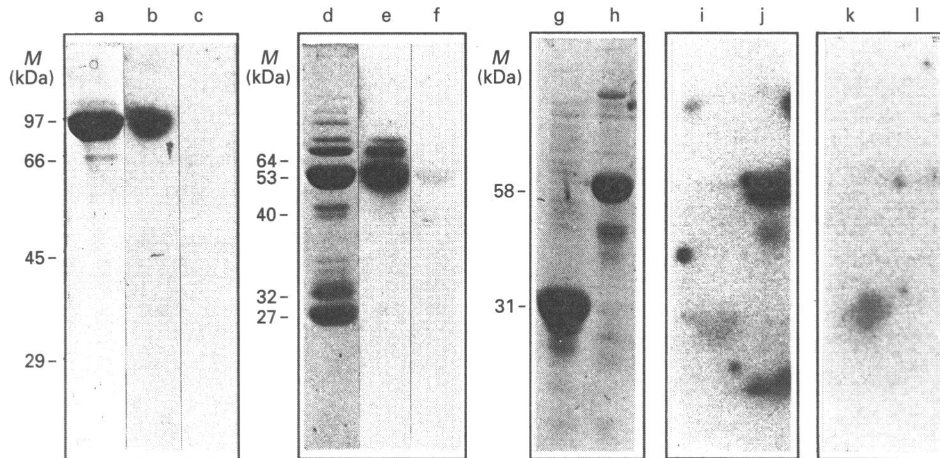

Figure 3 Binding of ^{125}-vinculin to α-actinin and α-actinin-derived polypeptides analysed using a gel-blot assay

(a–c) Purified chicken gizzard α-actinin (5 μg) analysed by SDS/PAGE was either stained with Coomassie Blue (a) or electroblotted to nitrocellulose (b and c) and the filters incubated with (b) ^{125}I-vinculin (1.5×10^{-8} M) and (c) ^{125}I-vinculin in the presence of a 100-fold molar excess of unlabelled vinculin. (d–f) A thermolysin digest of α-actinin (10 μg) analysed by SDS/PAGE and either stained with Coomassie Blue (d) or electroblotted to nitrocellulose (e and f) and the filters incubated with (e) ^{125}I-vinculin and (f) ^{125}I-vinculin in the presence of unlabelled vinculin as above. (g–l) Residues 1–269 (g, i and k) spanning the actin-binding domain of α-actinin, and residues 240–749 (h, j and l) spanning the central repeat region of α-actinin were expressed in and purified from *E. coli*. The purified proteins were analysed by SDS/PAGE and either stained with Coomassie Blue (g and h) or electroblotted to nitrocellulose (i–l) and the filters incubated with (i and j) ^{125}I-vinculin or (k and l) ^{125}I-vinculin in the presence of unlabelled vinculin. The position of molecular-mass (*M*) standards (kDa) relates to lanes a–c only. The molecular masses (kDa) of the major thermolysin fragments of α-actinin and the α-actinin polypeptides purified from *E. coli* as determined by SDS/PAGE are shown to the left of lanes d and g respectively.

Imamura et al., 1988). A larger value for the length of α-actinin from *Dictyostelium* has been reported (56 nm) (Wallraff et al., 1986). Vinculin, by contrast, showed only particles close to spherical in shape (Figure 2, panel B), with occasionally a 'tail' protruding from it. The diameter of the sphere was measured as 11.2 nm (S.D. 1.7 nm; $n = 21$). Previously published values have been in the range 8–12 nm diameter (Isenberg et al., 1982; Milam, 1985; Gimona et al., 1987). As in one of these previous reports (Isenberg et al., 1982), there was evidence in some cases of penetration of stain into the centre of the sphere (Figure 2, panel B, arrowed). This latter feature may not be surprising. Assuming the shape to be genuinely spherical, a particle of mass 117 kDa can be calculated to have a diameter of less than 8 nm if it were 'compact' to an extent typical of globular proteins. Hence some degree of penetrability of the structure is indicated. This suggestion is supported by the fact that the sedimentation coefficient of 6 S (Beck, 1989) would imply a molecular mass of only 100000 ± 9000, using the empirical equation based upon a survey of a large number of globular proteins by Squire and Himmel (1979). Hence it can be inferred that the 'swelling' of the monomer in solution is larger to a modest extent than that of typical globular proteins.

In mixtures of α-actinin (0.25 μM) and vinculin (0.43 μM) the spherical vinculin monomers were much easier to observe than the α-actinin rods (Figure 2, panel C). This, at first sight surprising, result may arise from the vinculin monomers having a much larger dimension in the plane of the substrate than the α-actinin rods, and hence giving rise to a depth of negative stain non-optimal for revealing the latter. Where distinctive structures were seen, these took the form of either a disc attached at the end of a rod (a 'lollipop'; Figure 2, panel C, arrowhead, and Figure 2, panel D) or of a rod with discs attached at each end (a 'dumb-bell', Figure 2, panel C, arrowed, and Figure 2, panel E). The lengths of these structures were estimated at 41.3 nm (S.D. 4.4 nm, $n = 11$) and 44.1 nm (S.D. 4.8 nm, $n = 16$) respectively. A direct interpretation of these structures is that the 'lollipop' is an α-actinin dimer with a vinculin monomer attached at one end, whereas the 'dumbell' is an α-actinin dimer with vinculin monomers attached at both ends. The numbers of 'dumbells' seen exceeded the number of 'lollipops' by a factor of about 2. Although it may be that the former are easier to discern, this result does differ by around two orders of magnitude from expectation on the basis of there being independent binding constants for the two putative vinculin-binding sites (see the Discussion section).

Analysis of the binding of ^{125}I-vinculin to α-actinin using a gel-blot technique

Binding of ^{125}I-vinculin to purified α-actinin resolved by SDS/PAGE and blotted to nitrocellulose filters has previously been demonstrated by Otto (1983), Wilkins et al. (1983) and Belkin and Koteliansky (1987), and is confirmed in the present study (Figures 3a and 3b). The specificity of binding was demonstrated by the fact that a 100 molar excess of unlabelled vinculin quantitatively inhibited the binding interaction (Figure 3c). To establish which region of the α-actinin molecule contains the vinculin-binding domain, the experiment was repeated using a theromylsin digest of α-actinin which contains a number of well defined fragments derived from the N-terminal actin-binding and the central spectrin-like repeat domains (Figure 3d and Figure 4a). ^{125}I-vinculin bound to the 64 kDa polypeptide containing the spectrin-like repeats and predicted to include the two EF-hand calcium-binding motifs, as well as to the 53 kDa polypeptide, which has the same N-terminus as the 64 kDa polypeptide (residue 266) and is predicted to extend up to the boundary of the first EF-hand (Figure 3e). Binding was again quantitatively inhibited by unlabelled vinculin (Figure 3f). In contrast, ^{125}I-vinculin did not bind to the 32 and 27 kDa polypeptides containing the actin-binding domain of α-actinin. These results place the vinculin-binding domain in α-actinin

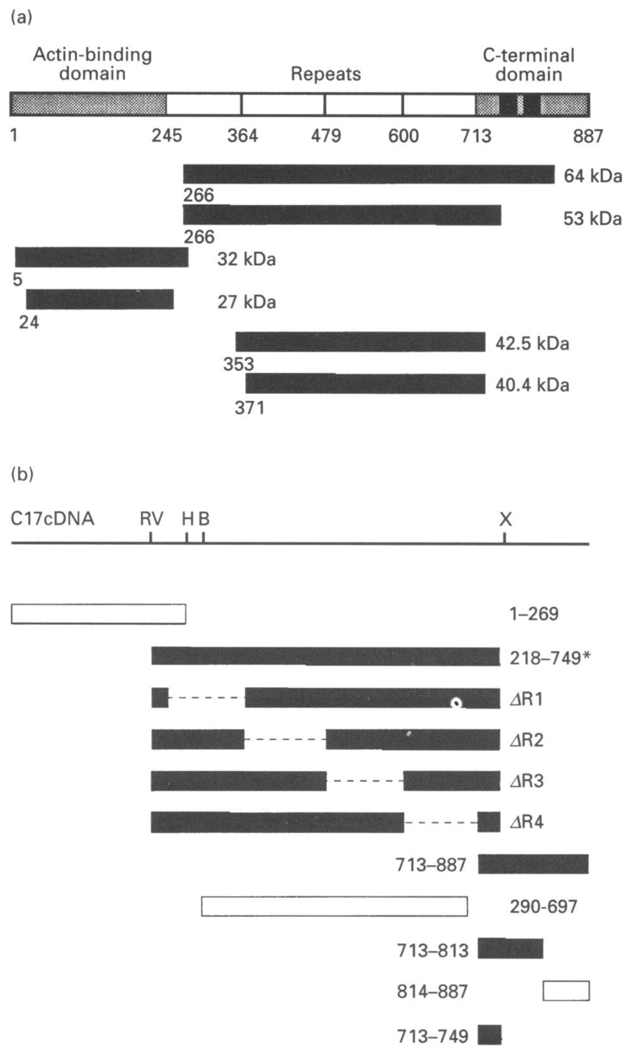

Figure 4 Alignment of α-actinin polypeptides produced by thermolysin digestion or by expression in *E. coli* with the domain structure of the α-actinin molecule

(**a**) The domain structure of chick smooth-muscle α-actinin in relation to the major α-actinin polypeptides liberated by digestion with thermolysin. Purified chicken gizzard α-actinin was digested with thermolysin, the liberated polypeptides resolved by SDS/PAGE (see Figure 3, lane d) and electroblotted to poly(vinylidene difluoride) membranes. Polypeptides revealed by staining with Coomassie Blue were excised, and the N-terminal sequence was determined. The position of the C-terminus of each polypeptide was estimated from its apparent molecular mass determined by SDS/PAGE. (**b**) The *Eco*RV (RV), *Hin*cII (H), *Bam*HI (B), and *Xmn*I (X) sites in the chick smooth-muscle α-actinin cDNA (C17) are shown relative to domain structure of α-actinin (**a**) and the positions of the α-actinin polypeptides expressed from this cDNA. Polypeptides ΔRI–ΔR4 each lack one of the spectrin-like repeats. Repeat boundaries were predicted by sequence alignments (Baron et al., 1987a,b; Blanchard et al., 1989). ■, α-Actinin polypeptides which bind ^{125}I-vinculin in the SDS/polyacrylamide gel-blot assay.

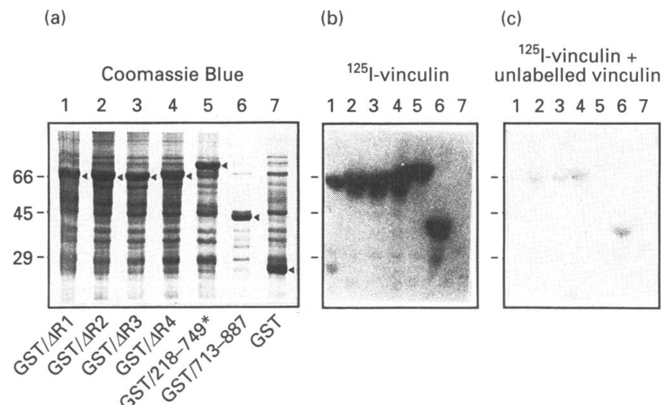

Figure 5 Binding of ^{125}I-vinculin to α-actinin fusion proteins analysed by using a gel blot assay

E. coli cell extracts expressing various α-actinin/GST fusion proteins were resolved by SDS/PAGE and the proteins (**a**) revealed by staining with Coomassie Blue or (**b** and **c**) electroblotted to nitrocellulose. Filters were incubated with either (**b**) ^{125}I-vinculin or (**c**) ^{125}I-vinculin in the presence of a 100-fold molar excess of unlabelled vinculin, and bound radiolabelled ligand was detected by autoradiography. The position of the fusion proteins in (**a**) is indicated with an arrowhead. Molecular-mass (M) standards (kDa) are shown to the left of each panel.

somewhere between residues 266 and the first EF-hand (residue 749).

In order to define further the vinculin-binding domain within α-actinin, we attempted to express various parts of the α-actinin molecule as GST fusion proteins in *E. coli* using the pGEX plasmid, a system which allows the rapid purification of soluble fusion proteins from cell lysates using glutathione–agarose beads. Initially, we expressed an *Eco*RV/*Xmn*I restriction-enzyme fragment of the partial chick smooth-muscle α-actinin cDNA C18 (Baron et al., 1987b), which encodes amino acid residues 218–749 (Figure 4b), but the protein was very sensitive to proteolysis between the GST and α-actinin portions of the molecule and could not be purified using affinity chromatography. However, the expressed α-actinin polypeptide liberated as a 58 kDa fragment could be purified by conventional chromatography (Figure 3h), and direct protein sequencing showed that its N-terminus was Thr-240. As predicted, this protein bound ^{125}I-vinculin, and binding was inhibited by unlabelled vinculin (Figures 3j and 3l). In contrast, a bacterially expressed polypeptide (residues 1–269) containing the actin-binding domain of α-actinin (Figure 3g) failed to bind ^{125}I-vinculin (Figures 3i and 3k). The results obtained using bacterially expressed α-actinin polypeptides are therefore identical with those obtained using proteolytic fragments of the α-actinin molecule.

To generate a stable fusion protein spanning α-actinin residues 218–749, we deleted the nucleotides encoding amino acid residues 238–241 from the *Eco*RV/*Xmn*I fragment using mutagenesis. The resultant fusion protein referred to as GST/218–749* was stable and could be purified by affinity chromatography. We therefore made four additional constructs in which each of the individual repeats (as defined by sequence alignment) were deleted (ΔR1, ΔR2, ΔR3, and ΔR4), as well as one (GST/713–887) encoding the C-terminal domain of the α-actinin molecule (Figure 4b). Somewhat surprisingly, all of these fusion proteins bound ^{125}I-vinculin in the gel-blot assay (Figures 5a and 5b), and binding was again inhibited by unlabelled vinculin (Figure 5c). GST alone did not bind ^{125}I-vinculin. The results raise the possibility that vinculin binding might be restricted to the small region of overlap between all of these α-actinin fusion proteins, i.e. residues 713–749, although it is also possible that there are several independent vinculin-binding sites within the α-actinin molecule.

To investigate these two alternatives, we made a series of additional cDNAs by PCR (Figure 4b). As repeat 1 was clearly not required for binding activity, the 5′ end of these cDNAs was fixed at a convenient *Bam*HI site within the repeat 1. The 3′ PCR

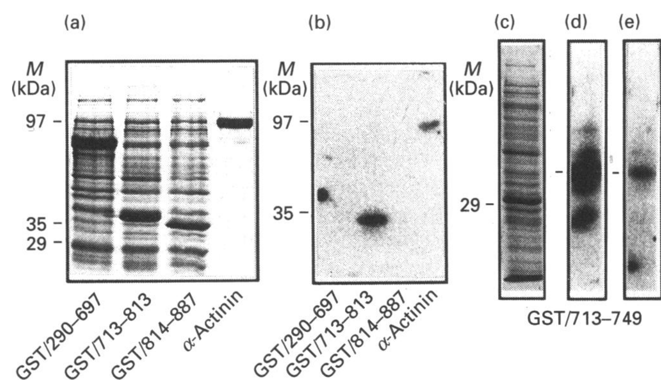

Figure 6 Binding of ^{125}I-vinculin to α-actinin fusion proteins analysed using a gel-blot assay: localization of the vinculin-binding domain to residues 713–749

Whole α-actinin or extracts from *E. coli* expressing α-actinin fusion proteins were resolved by SDS/PAGE and the proteins either visualized with Coomassie Blue (**a** or **c**) or electroblotted to nitrocellulose (**b**, **d** and **e**). Filters were incubated with ^{125}I-vinculin (**b** and **d**) or ^{125}I-vinculin in the presence of a 100-fold molar excess of unlabelled vinculin (**e**). Bound radiolabelled ligand was detected by autoradiography. The fusion proteins are the major proteins in each of the Coomassie-blue stained gels. Molecular-mass standards are shown on the left of each panel.

Table 1 Binding of ^{125}I-vinculin to α-actinin fusion proteins bound to glutathione–agarose beads

GST fusion proteins were purified from *E. coli* cell lysates using glutathione–agarose beads, and binding of ^{125}I-vinculin to beads containing equivalent amounts of fusion proteins was determined as described in the Materials and methods section. The assay was carried out in quadruplicate. Similar results were obtained in three separate experiments. Results are means ± S.D.

Fusion protein	^{125}I-vinculin bound (c.p.m.)
GST	6349 ± 1823
GST/1–269	6225 ± 1627
GST/218–749	30540 ± 1874
GST/713–887	29722 ± 1096
GST/713–813	28349 ± 1859
GST/814–887	5032 ± 1445
GST713–749	29986 ± 2174

primers contained an *Eco*RI site which allowed the PCR product to be force-cloned into the polylinker of the appropriate pGEX vector. Interestingly, a fusion protein spanning α-actinin residues 290–697 (Figure 6a) was devoid of ^{125}I-vinculin binding activity in the gel-blot assay (Figure 6b), indicating that the vinculin-binding domain is C-terminal to residue 697. In support of this conclusion, a fusion protein spanning residues 713–813 was able to bind ^{125}I-vinculin, whereas one spanning residues 814–887 was without activity (Figure 6b). The first EF-hand calcium-binding motif in chick smooth-muscle α-actinin is predicted to start at residue 750. It would seem unlikely that vinculin binds to this domain, and we therefore reasoned that the binding site must be located between α-actinin residues 713 and 749. In agreement with this prediction, a fusion protein spanning these residues (Figure 6c) retained ^{125}I-vinculin-binding activity (Figure 6d), and binding was inhibited by unlabelled vinculin (Figure 6e).

We next tested the ability of various purified α-actinin fusion proteins to inhibit the binding of ^{125}I-vinculin to α-actinin in the gel-blot assay. Densitometric analysis of the blots (results not shown) showed that fusion proteins spanning residues 218–749, 713–887 and 713–749 all produced > 83% inhibition of the binding of ^{125}I-vinculin to α-actinin, whereas a fusion protein containing the actin-binding domain (GST/1–269) or GST alone produced no significant reduction in binding. These results strongly suggest that the vinculin-binding site in α-actinin is contained within residues 713–749.

Binding of ^{125}I-vinculin to α-actinin fusion proteins adsorbed to glutathione–agarose beads

To check that the above results could be reproduced with α-actinin fusion proteins which had not been subjected to denaturing gel electrophoresis, binding of ^{125}I-vinculin to fusion proteins adsorbed to glutathione–agarose beads was monitored using a centrifugation assay. ^{125}I-vinculin bound to beads coated with fusion proteins spanning residues 218–749 and 713–887, whereas binding to beads coated with a fusion protein spanning residues 1–269 was no greater than to beads coated with GST alone (Table 1). Furthermore, ^{125}I-vinculin bound to fusion proteins spanning residues 713–813 and residues 713–749, but did not bind to a fusion protein spanning residues 814–887. The results are in complete agreement with those obtained using the gel-blot assay and support the conclusion that there is a vinculin-binding site within α-actinin residues 713–749.

DISCUSSION

We have determined the K_d for the interaction between α-actinin and vinculin under defined ionic conditions, with the assumption that the former contains two identical binding sites for the latter. A degree of vinculin dimerization has also been assumed based on the $\bar{M}_w$ of vinculin in solution determined in the present study, and the observations of Milam (1985) that vinculin self-associates through the C-terminal tail of the molecule. A computer model of the interaction has been constructed on this basis which enables us to estimate K_d by iteration. The value yielded (1.3×10^{-5} M) is higher than a previously published value (Wacchstock et al., 1987) of 2.2×10^{-6} M, but given a difference in ionic conditions and of methodologies between the two studies, and the lack of a consideration of vinculin dimerization in the earlier study, the difference in values may not be significant. However, electron microscopy shows a considerably higher proportion of α-actinin molecules with *two* vinculin molecules bound than would be predicted if the binding constants for the first and second binding event were identical; the possibility of co-operativity cannot be discounted. This would mean that our reported K_d value is an *effective* interaction constant, rather than one which refers explicitly to a single chemical interaction.

The results from electron microscopy are consistent with the presence of two vinculin-binding sites located at the extremities of the α-actinin dimer. In order to characterize these sites further, we have made extensive use of a gel-blot assay in which the binding of ^{125}I-vinculin to α-actinin and α-actinin polypeptides resolved by SDS/PAGE and blotted to nitrocellulose filters has been analysed. The specificity of this assay was established by the ability of a 100-fold molar excess of unlabelled vinculin to inhibit binding of the labelled vinculin. Similarly, pre-incubation of ^{125}I-vinculin with unlabelled α-actinin in solution also blocked binding of labelled ligand to α-actinin blotted to nitrocellulose. Others have used this assay to demonstrate an interaction between vinculin and α-actinin, although the authors either did

not attempt to demonstrate the specificity of the interaction (Wilkins et al., 1983; Belkin and Koteliansky, 1987; Pavalko and Burridge, 1991) or were unable to do so (Otto, 1983). Several factors must be taken into account when attempting to demonstrate inhibition of binding of labelled ligand in such assays, including the concentration of the labelled and unlabelled ligand, the K_d of the interaction, and the amount of binding protein. Considering an interaction with a K_d of 10^{-9} M and a concentration of radiolabelled ligand and binding protein of 10^{-8} M and 2×10^{-8} M respectively, one can calculate that a 10-fold excess of unlabelled ligand will reduce binding of labelled ligand by 80%. In contrast, when the K_d is of the order of 10^{-6} M (similar to that for the vinculin–α-actinin interaction), binding will only be reduced by 5% by a 10-fold excess of unlabelled ligand. Furthermore, the lower the concentration of radiolabelled ligand used, the greater the excess of unlabelled ligand required to inhibit binding. Such factors were not considered in any of the above studies.

Use of the gel-blot assay to study the binding of ^{125}I-vinculin to fragments of α-actinin generated either by limited proteolysis or by expression in *E. coli* has clearly established that the vinculin-binding site in α-actinin is localized in the region of the molecule containing the four spectrin-like repeats. Thus, ^{125}I-vinculin bound to the 64 kDa and 53 kDa fragments of α-actinin, which are derived from the protein by cleavage between residues 265 and 266 and more C-terminal sites, but it did not bind to the 32 kDa and 27 kDa fragments of α-actinin, which contain the N-terminal actin-binding domain. Similarly, ^{125}I-vinculin bound to a bacterially expressed fusion protein spanning α-actinin residues 218–749, but it did not bind to a fragment containing the expressed actin-binding domain (residues 1–269). In all cases binding was inhibited by unlabelled vinculin. These results are exactly the opposite of those of Pavalko and Burridge (1991), who reported that ^{125}I-vinculin bound to the actin-binding domain of α-actinin liberated by thermolysin, but not to the polypeptide containing the spectrin-like repeats. However, in these experiments the ^{125}I-vinculin bound much more strongly to the thermolysin used to cleave the α-actinin than it did to the liberated actin-binding domain, raising doubts about the specificity of the binding. Neither did the authors demonstrate that binding of ^{125}I-vinculin could be inhibited by unlabelled ligand. To verify the results we have obtained using the gel-blot assay, we sought an assay which avoided exposure of the α-actinin polypeptides to denaturing gel electrophoresis. Thus we studied ^{125}I-vinculin binding to α-actinin fusion proteins adsorbed to glutathione–agarose beads, using a simple pelleting assay. The results again clearly demonstrate that the vinculin-binding site in α-actinin is contained within the spectrin-like repeat region of the molecule, and there was no binding to the expressed actin-binding domain above background. By studying the binding of ^{125}I-vinculin to a number of additional fusion proteins, we have further defined the vinculin-binding site in α-actinin to between residues 713 and 749. This conclusion is based on the finding that fusion proteins containing this sequence bound ^{125}I-vinculin in the gel-blot assay and inhibited ^{125}I-vinculin binding to α-actinin in the same assay. Furthermore, ^{125}I-vinculin bound to these same fusion proteins adsorbed to glutathione–agarose beads. In contrast, fusion proteins lacking this sequence were not active in the above assays.

Whether the region of α-actinin containing the vinculin-binding site (residues 713–749) forms a distinct structural motif sandwiched between the end of repeat 4 (predicted to be residue 712) and the first EF-hand calcium-binding motif (which begins at residue 750) is not clear. Recent experiments on spectrin suggests that the phasing of the repeats is shifted by about 25 residues C-terminal to the boundaries predicted by multiple sequence alignments (Winograd et al., 1991). If this is also true for the phasing of the α-actinin repeats, then the vinculin-binding site might be contained within repeat 4.

The vinculin-binding site in chick smooth-muscle α-actinin (residues 713–749) is encoded by a single exon which also contains the coding sequence for the N-terminal region (residues 750–760) of the first EF-hand calcium binding motif (residues 750–782) (Waites et al., 1992). This exon is alternatively spliced to give rise to both the calcium-insensitive smooth-muscle isoform and a calcium-sensitive non-muscle α-actinin, which differ only between residues 750 and 760. The genomic organization of the chick skeletal-muscle α-actinin genes is identical in this region, again giving rise to an additional non-muscle isoform by alternative splicing (Parr et al., 1992). Interestingly, this region of α-actinin is highly conserved between isoforms and between species (Beggs et al., 1992), although we have not investigated whether other α-actinins bind vinculin or whether calcium has any effect on binding of vinculin to the non-muscle α-actinins.

The work was supported by the Medical Research Council. A.M. was supported by a Science and Engineering Research Council post-graduate training award. We are grateful to Dr. Paul Bolger and Mrs. Evelyn Roberts for help with the electron microscopy, and to Mr. Bipin Patel for technical assistance. We are grateful to Dr. C. R. Bagshaw for his help in modelling the interaction between α-actinin and vinculin.

REFERENCES

Arimura, C., Suzuki, T., Yanagisawa, M., Imamura, M., Hamada, Y. and Masaki, T. (1988) Eur. J. Biochem. **177**, 649–655

Baron, M. D., Davison, M. D., Jones, P. and Critchley, D. R. (1987a) J. Biol. Chem. **262**, 17623–17629

Baron, M. D., Davison, M. D., Jones, P., Patel, B. and Critchley, D. R. (1987b) J. Biol. Chem. **262**, 2558–2561

Beck, K. (1989) FEBS Lett. **249**, 1–4

Beggs, A. H., Byers, T. J., Knoll, J., Boyce, F. M., Bruns, G. and Kunkel, L. M. (1992) J. Biol. Chem. **267**, 9281–9288

Belkin, A. M. and Koteliansky, V. E. (1987) FEBS Lett. **220**, 291–294

Bennett, J. P., Zaner, K. S. and Stossel, T. P. (1984) Biochemistry **23**, 5081–5086

Blanchard, A., Ohanian, V. and Critchley, D. (1989) J. Muscle Res. Cell Motil. **10**, 280–289

Bretscher, A., Vandekerckhove, J. and Weber, K. (1979) Eur. J. Biochem. **100**, 237–243

Burridge, K. and Feramisco (1981) Nature (London) **294**, 563–567

Burridge, K., Fath, K., Kelly, T., Nuckolls, G. and Turner, C. (1988) Annu. Rev. Cell Biol. **4**, 487–525

Crawford, A. W., Michelsen, J. W. and Beckerle, M. C. (1992) J. Cell Biol. **116**, 1381–1393

Davison, M. D., Baron, M. D., Critchley, D. R. and Wootton, J. C. (1989) J. Biol. Macromol. **11**, 81–90

Duhaiman, A. S. and Bamburg, J. R. (1984) Biochemistry **23**, 1600–1608

Feramisco, J. R. and Burridge, K. (1980) J. Biol. Chem. **255**, 1194–1199

Fyrberg, E., Kelly, M., Ball, E., Fyrberg, C. and Reedy, M. C. (1990) J. Cell Biol. **110**, 1999–2011

Gimona, M., Furst, D. O. and Small, J. V. (1987) J. Muscle Res. Cell Motil. **8**, 329–341

Hemmings, L., Kuhlman, P. A. and Critchley, D. R. (1992) J. Cell Biol. **116**, 1369–1380

Imamura, M., Endo, T., Kuroda, M., Tanaka, T. and Masaki, T. (1988) J. Biol. Chem. **263**, 7800–7805

Isenberg, G., Leonard, K. and Jockusch, B. M. (1982) J. Mol. Biol. **158**, 231–249

Kuhlman, P. A., Hemmings, L. and Critchley, D. R. (1992) FEBS Lett. **304**, 201–206

Landon, F., Gache, Y., Touitou, H. and Olomucki, A. (1985) Eur. J. Biochem. **153**, 231–237

Luna, E. J. and Hitt, A. L. (1992) Science **258**, 955–964

Milam, L. M. (1985) J. Mol. Biol. **184**, 543–545

Mimura, N. and Asano, A. (1986) J. Biol. Chem. **261**, 10680–10687

Noegel, A., Witke, W. and Schleicher, M. (1987) FEBS Lett. **221**, 391–396

O'Halloran, T., Molony, L. and Burridge, K. (1986) Methods Enzymol. **134**, 69–77

Otey, C. A., Pavalko, F. M. and Burridge, K. (1990) J. Cell. Biol. **111**, 721–729

Otto, J. J. (1983) J. Cell Biol. **97**, 1283–1287

Parr, T., Waites, G. T., Patel, B., Millake, D. B. and Critchley, D. R. (1992) Eur. J. Biochem. **210**, 801–809

Pavalko, F. M. and Burridge, K. (1991) J. Cell Biol. **144**, 481–491
Podlubnaya, Z. A., Tskhovrebova, L. A., Zaalishvili, M. M. and Stefanenko, G. A. (1975) J. Mol. Biol. **92**, 357–359
Price, G. J., Jones, P., Davison, M. D., Patel, B., Bendori, R., Geiger, B. and Critchley, D. R. (1989) Biochem. J. **259**, 453–461
Rowe, A. J. (1984) in Techniques in Protein and Enzyme Biochemistry/Techniques in the Life Sciences (Tipton, K. F., ed.), BS106/1–37, Elsevier, Amsterdam
Rowe, A. J. (1988) Nature (London) **333**, 608
Sambrook, J., Fritsch, E. F. and Maniatis, T. (1989) Molecular Cloning: A Laboratory Manual, Cold Spring Harbor Laboratory Press, Cold Spring Harbor, NY
Smith, D. B. and Johnson, K. S. (1988) Gene **67**, 31–40
Squire, P. G. and Himmel, M. (1979) Arch. Biochem. Biophys. **196**, 165–177
Suzuki, A., Goll, D. E., Singh, I., Allen, R. E., Robson, R. M. and Stromer, M. H. (1976) J. Biol. Chem. **251**, 6860–6870

Received 8 November 1993/31 January 1994; accepted 2 February 1994

van Holde, K. E. and Baldwin, R. L. (1958) J. Phys. Chem. **62**, 734–740
Wachsstock, D. H., Wilkins, J. A. and Lin, S. (1987) Biochem. Biophys. Res. Commun. **146**, 554–560
Waites, G. T., Graham, I. R., Jackson, P., Millake, D. B., Patel, B., Blanchard, A. D., Weller, P. A., Eperon, I. C. and Critchley, D. R. (1992) J. Biol. Chem. **267**, 6263–6271
Wallraff, E., Schleicher, M., Modersitzki, M., Rieger, D., Isenberg, G. and Gerisch, G. (1986) EMBO J. **5**, 61–67
Way, M., Pope, B., Gooch, J., Hawkins, M. and Weeds, A. G. (1990) EMBO J. **9**, 4103–4109
Winograd, E., Hume, D. and Branton, D. (1991) Proc. Natl. Acad. Sci. U.S.A. **88**, 10788–10791
Wilkins, J. A., Chen, K. Y. and Lin, S. (1983) Biochem. Biophys. Res. Commun. **116**, 1026–1032
Witke, W., Hofmann, A., Koppel, B., Schleicher, M. and Noegel, A. A. (1993) J. Cell. Biol. **121**, 599–606